# Mapping paleoflooded and emerged areas around lake marshes (Tablas de Daimiel, Spain) using hyperspectral DAIS 7915 and ROSIS Spectrometer data

[a] RIAZA, A., [b] GARCIA MELENDEZ, E., [b] SUAREZ, M., [c] HAUSOLD, A., [c] BEISL, U., and [d] VAN DER WERFF, H.

[a] Instituto Geológico y Minero de España, Madrid, Spain, email: a.riaza@igme.es
[b] Departamento de Geología, University of Salamanca, Salamanca, Spain
[c] German Aerospace Research Establishment, Remote Sensing Data Centre, Oberpfaffenhofen (Bayern), Deutschland
[d] International Institute for Aerospace Survey and Earth Sciences, Enschede, The Netherlands

## ABSTRACT

Open-system lakes developing marshes are sensitive environments to climate changes. Mineralogical climate markers such as gypsum and dolomitized carbonate are spatialy traced using hyperspectral imagery. Climate-dependent saline soils, carbonate , organic matter and iron oxide crusts have been mapped along different stages of flooding and emersion in the past 2000 years using DAIS and ROSIS spectrometer data. Spectral behaviour interacting and masking from various mineralogical components are described on laboratory spectra. Sediments permanently exposed to the atmosphere dehydrate and oxide, developing different mineralogical associations. Increase of the iron oxide/hydroxide rate and decarbonation can be spectrally followed on the sands framing the nowadays marshy area. A general outline of the past pools is drawn on the area surrounding the actual marsh, providing priceless data to use in further paleoclimate limnological research and in the development of new techniques for that research.

**Keywords:** hyperspectral, geology, paleoclimate, limnology.

## 1 INTRODUCTION

The Las Tablas de Daimiel Natural Park frames a lake at the head of the river Guadiana draining to the Atlantic, settled in the large plain of La Mancha in central Spain (fig.1). This continental dry plain is subject to a Mediterranean climate with dry summer and winter and relatively short rainy seasons in spring and autumn. Periods of drought are recurrent within the lapse of five years. It is a wetland with a linear morphology associated to an alluvial plain (Casado and Montes, 1995), resulting from two main interacting processes: the overflooding of the rivers Cigüela and Guadiana, which join at the Tablas de Daimiel. And second, the natural discharge of the underlying aquifer, through upwelling water at points locally termed "ojos" (eyes).

The recent sedimentological record of the Quaternary deposits in the area points to recent harsh paleoenvironmental conditions (2500-2300 years before present) with diminishing humidity and lowering of groundwater levels (García Antón et al, 1986). Intensive use of groundwater for cereal crop irrigation has produced a serious descent on the groundwater level and cover, an already irreversible environmental problem. Today the Tablas de Daimiel has long since ceased to be an upwelling groundwater area and has instead become a big pool of artificial water inflow (Llamas, 1998).

Lakes are environments particularly sensitive to climate changes, both actual and paleoclimates. Open system lakes fed by groundwater and seasonal runoff show a fluctuating shoreline.

The most recent sediments hosting the wetland are holocene sands (Rodríguez García, 1998) arranged on several morphological units descending towards the marshy area. On a semi-arid climate, the well ventilated and open sand deposits which are emerged, easily lose water. The iron bearing minerals decrease in hydroxides (goethite) to gain anhydrous ferric oxide (hematite) (Duchaufour, 1984). As the wetland recedes, the whole system is demantled down towards the river. Four morphological units can be traced through the imagery on the everemerged sands surrounding the marsh, based on their different height from the coastline, confirmed by fieldwork and aerial photography interpretation. These units are related to terraces, eolic deposits and desiccated areas, and appear as both continuous and remanent sparse encased surfaces showing different stages of landscape development. The

Presented at the 3rd EARSeL Workshop on Imaging Spectroscopy, Herrsching, 13-16 May 2003

earlier units are topographically high, and show a bright strong brown colour to the eye because of the comparatively higher hematite contents.

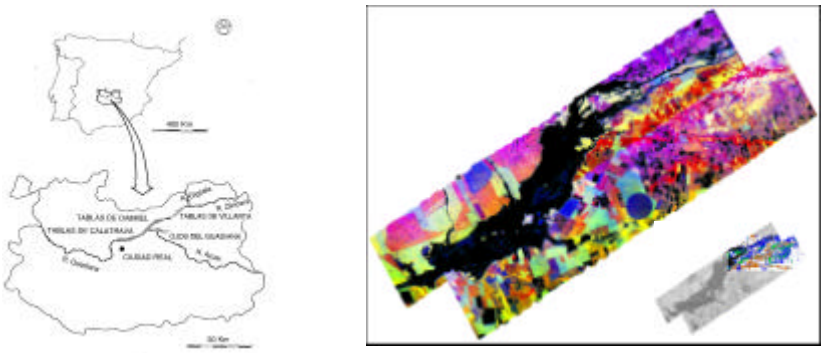

**Figure 1.** Geographical location of the Tablas de Daimiel wetland and natural park. False colour composite with Principal components 1 (red), 2(green) and 3 (blue) computed from the six thermal infrared DAIS channels on the flight line mosaic after masking water and dense vegetation. Indication of the northeastern area selected for mapping.

Organic sediments (peat) occur when the shallow channels excavated by the rivers overflow the adjacent floodplains with sediments loaded with clay, silt, sulphate, calcium and in lesser amounts, magnesium and chlorides. This favours the development of marshes on permanently flooded areas with abundant vegetation, where organic matter deposits occur. During the periods of draught, the groundwater level deepens, and the sediments are exposed developing saline soils with gypsum and dolomitization of carbonate. Water level fluctuations in open-system lakes cause much reworking of sediment in the nearshore zone (Allen and Collinson, 1978, in Reading, 1978).

Space and airborne imagery depicts subtle variations in the reflectance properties of desert surfaces, which are indicative of changes in mineralogical composition. The intensity of the red colour of sands in Namibia (Logan, 1960) has been used as an indication of age in the dunes. In Australia, the intensity of dune reddening resulted in information about the distance from the sand source area (El Baz, 1978; El Baz and Prestel, 1980). Desert loess is studied using spectral mixture algorithms (White et al, 2000) helping its use as a paleoclimate record.The spectral behaviour of iron bearing minerals have been long studied because of their wide presence on lunar rocks (Hunt et al, 1971b, Wickersheim and Lefever, 1961). Limonitic alteration was one of the first features attracting the attention of geological remote sensing (Rowan et al 1976, 1977, Abrams et al 1977, Hunt and Ashley 1979, Segal 1982,1983, Townsend 1987). Weathering processes produce the same minerals as hydrothermal alteration processes (Buckingham and Sommer 1983), and mask the spectral response of underlying rocks with coatings and internal mineralogical transformations (Lyon 1997).

The presence of hematite coatings on individual grains has been given as the cause of red colour in desert sands (Walker,1967). Recent studies indicate that the coating on sand grains is composed of kaolinite with powdery hematite, thus linking such reddening to desert varnish (Potter and Rossman, 1977). Kaolinite in the coating is believed to originate as dust that percolates through the sand and adheres to the surfaces of the grains. The coating on quartz grains increases in thickness with the location, as well as the reddening of the sands increases with the transport distance (McCay et al, 1980), suggesting that the quartz grains acquire the coatings during transport. Therefore, the reddening property can be used to determine the relative ages of colour zones in the same sand field.

Recent use of spectral response of iron bearing minerals in fluvial sediments is addressed to map the contamination of mine waste disposals (Farrand, 1997) using hyperspectral imagery. Traditional studies on laterite soils are conducted using the relative amount of iron oxides and hydroxides (Madeira et al, 1997) in humid rainforest climate.

Carbonate are minerals forming during lacustrine and weathering processes on arid climate. Numerous spectral studies refer to carbonate as a petrographic tool (Hunt and Salisbury, 1971a; Gaffey, 1986; Crowley, 1986). Carbonate absorptions and chromaticity values were statistically evaluated (Jarmer et al, 2000) establishing a model to be transferred to hyperspectral image analysis.

Weathering of rock and soil surfaces responsible for the exterior mineral mixtures mainly contributing to the spectral response detected by remote sensors has collected attention among the remote sensing geological

community (Pontual, 1987; Amos and Greenbaum, 1989; Younis et al, 1997; Lyon, 1997; Riaza et al, 1995, 1997, 2000, 2001,2002, 2003).

Different stages on weathering products and textures have been used for relative dating of lava flows of the same chemical and mineralogical composition with thermal infrared data (Kahle et al, 1988; Abrams et al, 1991). Using the same approach in a large scale, geomorphologic regional considerations can be made.

The mixtures of iron and clay minerals produced by weathering alteration associated to posthercynian erosion paleosurfaces in the Duero Basin (Central Spain) developed under different paleoclimates have been mapped using thematic mapper imagery (Riaza et al, 1997). Different image processing procedures helped to model sediment patterns on various stages of the evolution of the sedimentary basin (Riaza et al, 1995, 1997, 2000). The effects of weathering processes on the spectral response of rocks exposed to the atmosphere have been evaluated both on sedimentary and igneous rocks on laboratory spectral measurements in the visible and nearinfrared (Riaza, 1992; Townsend, 1987; Rivard et al, 1992 ). Iron bearing minerals, gypsum, carbonate and clays, have been used as the main mineral spectral references for the geological mapping of a carbonate area in the desert of Israel using the hyperspectral airborne spectrometer DAIS 7915 (Riaza et al, 1998) and alluvial fans in a semi-arid environment (García-Meléndez et al, 2000). Iron bearing minerals, gypsum, carbonate and clays, have been used as the main mineral spectral references for the geological mapping of a carbonate area in the desert of Israel using the hyperspectral airborne spectrometer DAIS 7915 (Riaza et al, 1998).

Prior work has been focused on the spectral behaviour of playa evaporites both in the visible and nearinfrared (Crowley, 1991, 1993) and thermal infrared (Crowley, 1996). The influence of organic matter on soil colour is a long experienced relationship in spectrometry (Shields et al, 1968, Leone and Escadafal, 2001; Mathieu et al, 1998). Saline soils are recurrent on remote sensing studies because of their relationship with anthropic irrigation uses (Dehaan and Taylor, 2002; Koch et al, 2000). Various spectral libraries of minerals and rocks have been built, which are now in the public domain and well known by the geological community (Clark et al, 1993; Grove et al, 1992; Salisbury et al, 1992).

Areas flooded by water in the past which are nowadays exposed to the surface in the Tablas de Daimiel have changed the mineralogical and spectral aspect of the underlying Holocene sands, the most recent deposit hosting the wetland. The colour of the sand is darkened to grey, by influence of large amounts of organic matter deposited at the bottom of the flooded area. Meanwhile, peat and saline deposits are developed. Gypsum and carbonate precipitate (Arauzo et al, 1996), and new clays such as palygorskite and sepiolite occur. Such mineralogical changes can be spectrally detectable on the imagery.

## 2 METHOD

DAIS 7915 and ROSIS Spectrometer data were recorded on July 2000, aiming to minimum vegetation vigour and maximum soil exposure. The spatial resolution of 5 m for DAIS and 2 m for ROSIS was ensured at a flying altitude with maximum signal to noise ratio.

Non-coherent noise was corrected after in-flight calibration for DAIS (Strobl et al, 1996) to remove the sensor sensitivity effects on the 79 DAIS channels. Different spectral imaging processing tools were tested on atmospherically corrected data using a midlatitude summer profile (Richter, 1996; Richter et al, 2002) using field spectra from dark and light targets. ROSIS data with 115 channels in the visible 430-860 nm wavelength range, were corrected using a different procedure (Gege et al, 1998). Both sensors operated simultaneously at the same flight altitude. As a consequence, the area covered by ROSIS is a narrow belt centered along the DAIS central flightline. The main interpretation procedures were focused on DAIS data. Particular nuances in the visible were contrasted with ROSIS data, with a 4 nm spectral resolution and 2 m spatial resolution compared to the 5 m DAIS spatial resolution.

Field spectra were collected for thematic analysis on geologically representative targets to be used for interpretative image processing with a GER Spectrometer. Non consolidated soil samples were collected at different stages during the interpretation of the imagery lead by hyperspectral image processing suggestions on mineralogy and sedimentology. Laboratory spectra were run on field soil samples using a Perkin-Elmer Lambda 6 Spectrometer in the visible and nearinfrared provided with an integrating sphere. Non consolidated rock samples were dry-sieved before measurement.

X-ray diffraction analysis was performed on selected non-consolidated rock samples to confirm field observations regarding mineralogical contents. Laboratory measurements were made on powdered samples after XRD aiming to ascertain spectral features which might appear on fine grained samples after separation of the clay fraction.

Image processing was conducted using ENVI hyperspectral modules and reference spectral libraries.

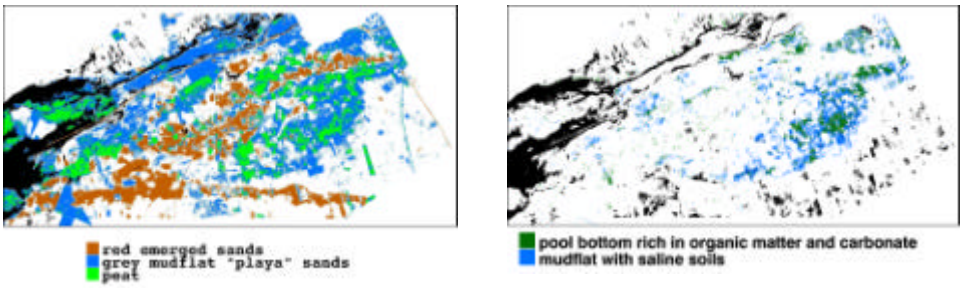


**Figure 2.** Left: Geological map composed from DAIS images indicating the main morphological units in flooded areas. Right: Map built using Spectral Angle Mapper on the grey mudflat "playa" sands on the 72 VIS-NIR DAIS channels using six selected field spectra taken with a GER spectrometer (fig.3). The deeper areas of the paleopool richer on organic matter and carbonate are isolated from the flooded mudflats on a fluctuating shore developing saline soils.

## 3 DIGITAL IMAGE PROCESSING

DAIS images were processed aiming to separate different sediments and minerals indicative of geological processes both of palustrine and fluvial environments. Mosaics were composed with the two scenes for panoramic view of the area, and for selection of areas of interest (fig.1). Masks were built for densely vegetated areas using channels 17 and 13 for a red/nearinfrared ratio. Masks for water were also built using value 26 on channel 1 as threshold. A false colour composite with channels 19, 6 and 53 (BRG) was selected gathering both information on the three DAIS detectors on the visible and nearinfrared, and wavelength ranges which are critical for known reflectance absorptions diagnostic of minerals present in the area.

The six thermal infrared channels were used for a primary estimation of lithological variety (Riaza et al, 1998) (fig.1). Both Principal Components and Minimum Noise Fraction Transforms were useful identifying the main lithological regions indicating further hyperspectral image processing. Masks were built using selected minimum noise fraction transforms from thermal infrared channels to isolate different areas on the sands (fig.1). Pixel Purity Index and n-dimensional analysis were run on selected masked areas, helping to understand the spectral meaning of the various statistical populations among the sands (Boardman et al, 1993; Boardman and Kruse, 1994).

Illumination Angle Effects jeopardised any subtle hyperspectral analysis. Image processing procedures were repeated for individual scenes and subsets, and maps were produced composing final results for the same geological units.

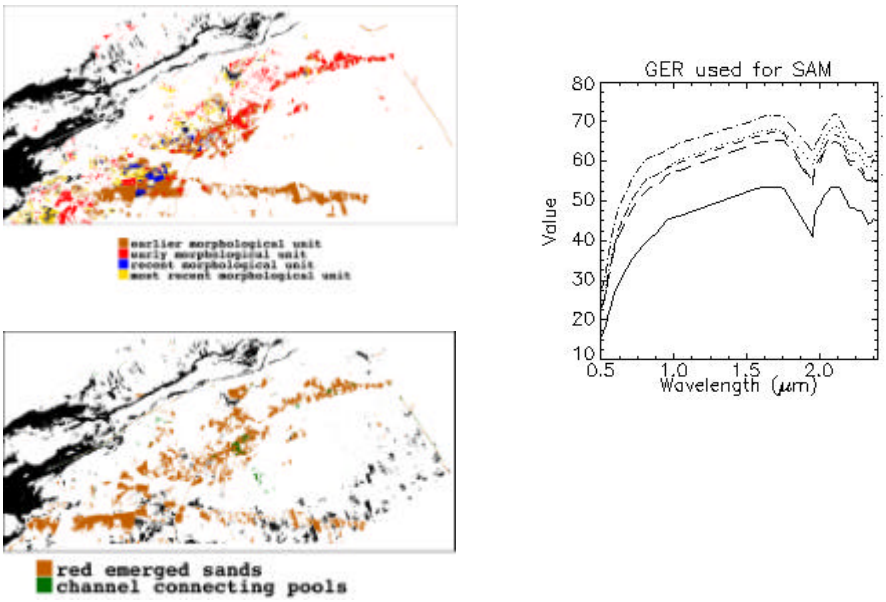


**Figure. 3.** Up: Geological map composed from DAIS images indicating the main morphological units. Down: Map built using Spectral Angle Mapper on the red emerged sands on the 72 VIS-NIR DAIS channels using six selected field spectra taken with a GER spectrometer . A channel connecting the two main paleopools is shown. Right: Field spectra taken with a GER spectrometer selected as showing better different geological units.

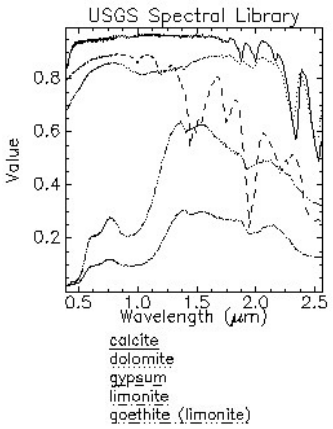


**Figure 4**. Spectra of the main minerals present on the sediments of the area of study related to palustrine processes and dehydration of sands exposed to the atmosphere (United States Geological Survey Spectral Library).

Field spectra taken with a GER Spectrometer were used with Spectral Angle Mapper (Kruse et al, 1993). Spectra showing iron absorption features were grouped into a library, and spectra showing carbonate absorptions were included into a different library.

Spectral Angle Mapper was run on the 72 VIS-NIR DAIS channels on independent areas masked for the three main sandy areas: red emerged sands, depressions with organic matter, and flooded mudflats temporarily exposed developing saline soils (fig.3). The same procedure was used with the iron absorption library using only the 29 VIS DAIS channels, and the library with spectra showing carbonate absorptions was used to compute maps on the 2000-2500 nm wavelength range. Six representative spectra were selected after several attempts, giving better spatial outline of geological paleoflooded regions.

The resulting maps were quite noisy when using a reduced number of channels, so that only maps computed with the 72 VIS-NIR channels were used for analysis. All results were very similar on areas drawn, coinciding with the spectral signatures coming from Pixel Purity Index and n-dimensional Analysis. Spectral Angle Mapper was more sensible showing the deeper flooded areas richer both in carbonates and organic matter.

When using Spectral Angle Mapper on the red emerged areas, no main differences were shown among the red sands (fig.3), apart from a possibly connecting channel among the two main paleopools, which is spectrally prominent. This connecting very shallow channel was not obvious on the prior analysis using Minimum Noise Fraction Transforms, Pixel Purity Index and n-dimensional analysis.

Laboratory spectra of nonconsolidated rock samples pointed to channels 33 (1520-1544 nm, gypsum), 34 (1565-1575 nm (gypsum), 40 (1777-1757, gypsum), 59 (2229-2225 nm, illite), 60 (2230-2240 nm, illite), 61 (2250-2253, gypsum, illite, palygorskite) and 64 (2298-2297 nm, sepiolite, dolomite) as critical showing absorptions related to minerals in the area (fig.4). Channels 41, 42 and 70 mineralogically sensitive to gypsum, goethite, calcite, illite and iron oxides, were rejected because of low signal quality. Hyperspectral image processing is impossible on this reduced number of channels, and more conventional image processing gives noisy results. However, useful hints came from colour composites built with minimum noise fraction transforms 213 (blue, red, green) and principal components 214 (blue, red, green) from such channels.

The same procedure was used for ROSIS, elaborating parcial maps to contrast with DAIS results.

## 4 LABORATORY SPECTRA

### 4.1 Flooded areas

Visual and mineralogical analysis of the fluvio-lacustrine system of the Tablas de Daimiel depicts a sulphate and carbonated water solution, being chloride absent. Intensive agricultural practices have destroyed any crusts which might have developed on the surface. Saline minerals are unstable mineralogical components, relying on subtle variations of temperature and humidity to precipitate or dissolve. Such physical parameters may change during daytime. Therefore, saline minerals excluding gypsum have not been used on the spectral interpretation, nor are crusts of any sort expected to be recorded by the imagery.

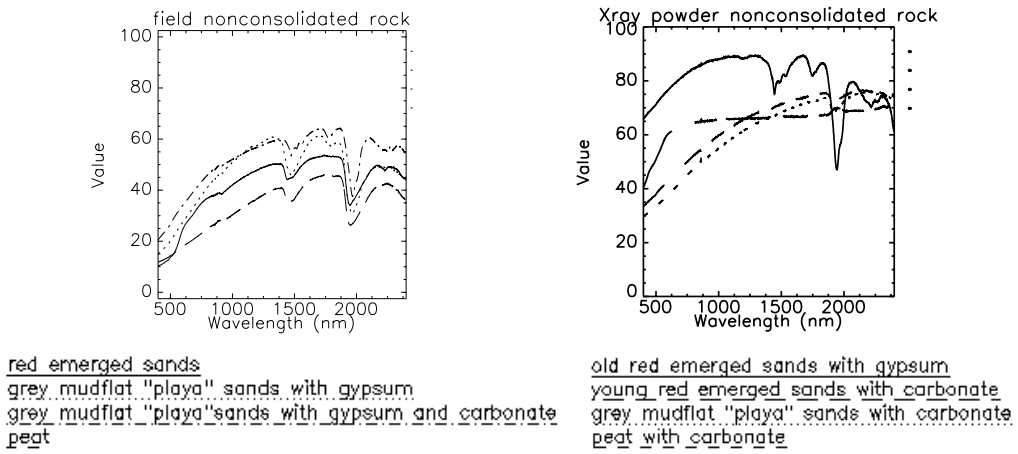


**Figure 5.** Left: Laboratory Spectra from field nonconsolidated rock samples using a Perkin Elmer Lambda 6 Spectrometer on representative morphological units, with expression of the minerals whose absorption features are present. Right: Laboratory Spectra from powder after X Ray Diffraction Analysis from field nonconsolidated rock samples, using a Perkin Elmer Lambda 6 Spectrometer on representative sediments, with expression of the minerals whose absorption features are present.

The spectral response of mudflats around the former wetland are mineralogicaly dominated by gypsum and carbonate, whether calcite or dolomite (fig.5). Increasing dolomite contents would indicate an intensification of palustrine processes. Clays are not widely present in the area, nor does laboratory mineralogical analysis detect them.

Laboratory spectra of peat is dominated by the presence of gypsum on typical shapes with minimum at 1477, 1520, 1565 and 2250 nm (Clark et al, 1992) (fig.5). The presence of carbonate appears as a weak 1975 nm minimum. Sepiolite and mainly dolomite are detected by the 2298 nm.

The grey sands, which have been once flooded by water present a dolomite 2298 nm minimum, absent on the rest of the sands (fig.5). XRD have revealed the presence of nesquehonite, a magnesium carbonate common as secondary mineral in saline playa deposits with high Mg/Ca ratios and high Mg concentration in water (Kelts and Hsü, 1978). The presence of dolomite is indicative of organic matter degradation, whether by oxidation liberating sulphur, or by increase of Mg in the system from runoff.

The spectral response of gypsum dominates grey sands, along with dolomite (fig.5). The displacement of a minimum from 1940 to 1970 nm indicates the transition from the temporarily flooded mudflat to the everemerged sands only subjected to reddening by iron coatings developed by exposure to the atmosphere. Spectra on powdered samples for X-ray diffraction analysis only display the gypsum absorption features when present. However, carbonate has been reported on the same samples. Gypsum dominates and hinders spectrally the presence of carbonate, both on soil samples and clay-size powdered samples (fig.5). The presence of gypsum on the grey sands increases geographically towards the river, indicating a likely progressive water salinity in comparatively recent times.

Peat, in spite of the high contents of organic matter, records spectrally the presence of gypsum (fig.5). High contents of organic matter obliterates any spectral response from iron minerals (Galvao and Vitorello, 2001). Presence of carbonate is shown by spectra run on clay-size powdered samples for X-ray diffraction analysis (fig.5).

Carbonate is widespread throughout the area, both in emerged and flooded areas. Imagery is quite noisy on the nearinfrared to be able to show carbonate-related absorption, relatively weak on the laboratory spectra. However, the topographically low areas where water was deeper and rich in gypsum should pop on the nearinfrared, even if the hyperspectral profiles on DAIS imagery do not depict a clear spectral response due to the low energy available for the fourth detector on the 2000-2500 nm wavelength range.

## 4.2 Emerged areas

The Holocene red sands surrounding the Tablas de Daimiel wetland are sediments composed of sand with quartz as a principal component. Clays are responsible for the 1438 nm minimum. Goethite contributes with a weak 1943 nm minimum and illlite to the 2229-2230 nm and weak 2370 nm minimum (fig.6). X-ray diffraction analysis

showed no presence of clays on the red sands, but rather and widespread carbonate. Spectra run on clay size powder from soil samples showed the presence of carbonate on most red sands.

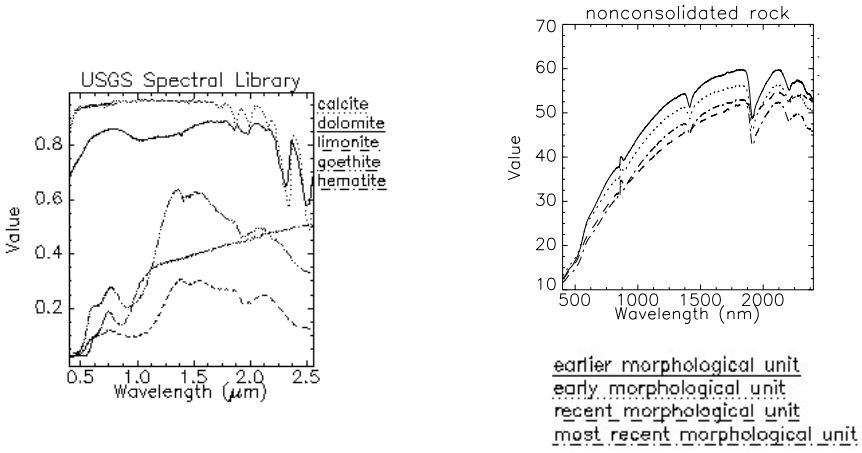


**Figure 6.** Left: Spectra of the main minerals present on the sediments of the area of study related to dehydration of sands exposed to the atmosphere (United States Geological Survey Spectral Library). Right: Laboratory Spectra from field nonconsolidated rock samples using a Perkin Elmer Lambda 6 Spectrometer on representative morphological units, with expression of the minerals whose absorption features are present.

Strong brown colour (Munsell, 1990) occurs on earlier and topographically highest early units rich in hematite resulting on deeper iron absorptions in the visible and higher overall reflectance. Dark brown colour on recent units is associated to lower overall reflectance and more abundant iron hydroxide in the mineral mixture.

The early topographically higher morphological units rich in hematite display a smooth absorption at 850 nm because of the presence of ferric cation (7.5YR 5/8, strong brown; 7.5YR5/6 strong brown-brown) (Hunt et al, 1971b). Hematite is also shown by the inflexion point at 548 nm in the visible (fig.6). The recent units (10yr 4/3, brown-dark brown; and 10yr 4/6, dark yellowish brown) display a less steep straight line response in the visible, including a lower overall reflectance, due to the more abundant iron hydroxide. Recent units also show a more flattened shape at 2300 nm due to carbonate (Hunt and Salisbury, 1971a).

Carbonate is widespread throughout the area, both in emerged and flooded areas. Imagery is too noisy on the nearinfrared to be able to show carbonate-related absorption, which is relatively weak on the laboratory spectra. Hyperspectral profiles on DAIS imagery do not depict a clear spectral response due to the low energy available for the fourth detector on the 2000-2500 nm wavelength range, but trends of more abundant carbonate are suggested on the early hydrated units.

## 5 DAIS SPECTRAL RESPONSE

DAIS images present a distinguishing response from once flooded and everemerged areas (fig.7).

### 5.1 Flooded areas

In the nearinfrared, the most distinguishing feature is the presence of a narrow absorption at 2.1 μm on areas which were flooded. Both bloedite $Na_2Mg(SO_4)_2.4H_2O$, calcite and dolomite can be responsible.

DAIS imagery show differences inside the flooded areas due to the variable contents on organic matter, gypsum and saline minerals (fig.4,7). The deeper hydrologically closed areas, where standing water persisted longer to develop marshes and to precipitate organic matter in detectible amounts, seem to be richer also in gypsum. When the groundwater level lowers, marshes are exposed to the atmosphere developing saline soils.

Preliminary analysis on DAIS imagery does not show distinctive absorptions among the mapped units, but Spectral Angle Mapper using selected field spectra depicted subtle spectral variations (fig. 3). A depression on 2.3 μm is present on both peat and saline mudflats, whether due to gypsum or carbonate (fig.7). The overall reflectance is lower on the areas longer flooded due to more abundant organic matter.

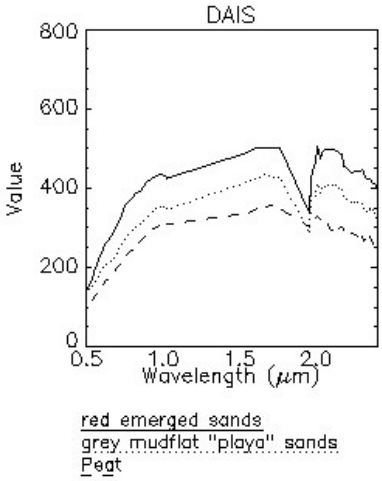


**Figure 7**. Z profiles from DAIS images from areas representing sedimentary units on maps built using digital image processing in the visible and nearinfrared in flooded areas ( fig.2).

## 5.2 Emerged areas

All the emerged areas, whether sand deposits or continental aprons or fluvial deposits, show depressions in the visible due to the presence of iron bearing minerals.

The wide depression on red everemerged sands is more pronounced, consistent with their strong brown colour (fig.8,3). In all of the mapped units, early emerged sands display the highest overall reflectance. The areas which were once flooded are less expressive on the visible.

The areas which are emerged display a shoulder centred between 2.2-2.3 μm non-existent on the flooded areas. This might suggest abundance of clays, which is not confirmed by XRD mineralogical analysis or by sedimentological expectations. Widespread carbonate can also contribute to this spectral feature.

Several systems of reddish sands have been spectrally identified based on different iron minerals related to variable time of exposure to the atmosphere and weather conditions. Four morphological units can be distinguished by intensity of reddening directly related to age (fig.3,8). The intensity of redness in semi-arid environments is related to the increasing hematite contents (Duchaufour, 1984) by loss of water in the environment. Goethite decreases in the iron bearing mineral mixtures with increasing dryness.

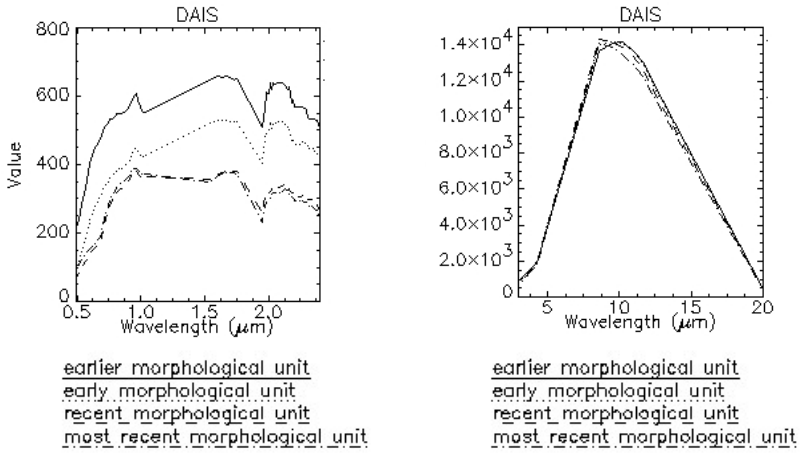


**Figure 8.** Left: Z profiles from DAIS images from areas representing sedimentary units on maps built using digital image processing in the visible and nearinfrared on emerged areas (fig.3). Right: Z profiles from DAIS images from areas representing sedimentary units on maps built using digital image processing in the thermal infrared on emerged areas.

Such mineralogical changes are spectrally recorded by the imagery. The topographically upper and early morphological units show a shoulder on 0.85 μm due to the ferric ion from hematite (Hunt et al, 1971b). This is not present on the lower and recent morphological units.

The two recent morphological units display a smooth depression between 0.70-0.74 μm due to the iron hydroxide goethite (Hunt et al, 1971b). The presence of OH groups is not spectrally recorded by iron hydroxides, nor does the imagery show them on the recent less dehydrated units (Hunt et al, 1971b).

Carbonate is also obvious on the two recent morphological units by a subtle 2.3 μm absorption or flattened shape in comparison with spectra from hematitic surfaces. This absorption is not present on the two earlier units, which have been exposed enough time to be decarbonated.

The thermal infrared channels from DAIS images display a varied spectral response for the four morphological units (fig.8). The recent units rich in hydroxides show a higher emmissivity at 8.58 μm lowering comparatively to the older units at longer wavelength ranges.

## 6 ROSIS SPECTRAL RESPONSE

ROSIS data display a similar pattern of geological units when following the same digital image processing procedure used for DAIS (fig.9). Improved spatial resolution increases the spectral variability particularly on red emerged sands. Spectra do not display a very obvious iron absorption feature, due to the atmospherical correction system.

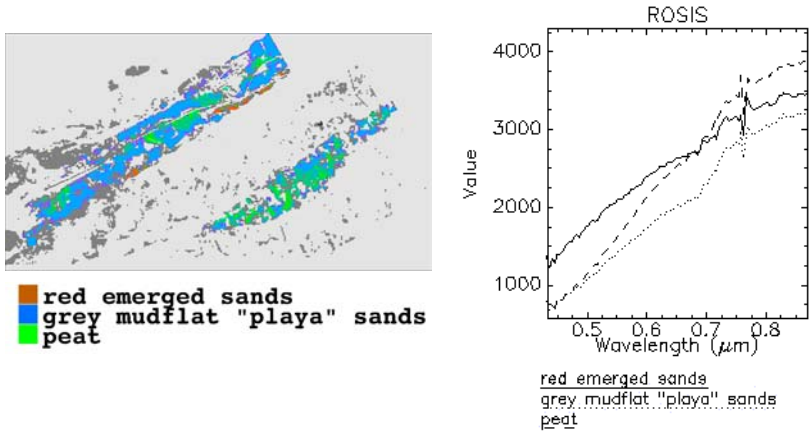


**Figure 9.** Left: Map built from ROSIS data using a similar procedure to former DAIS data, overlying over DAIS images, representing the main sedimentary units. Right: Z profiles from ROSIS images from areas representing sedimentary units on maps built using digital image processing.

## 7 CONCLUSIONS

Hyperspectral imagery has been able to distinguish paleoflooded areas related to a receding wetland due to differential mineralogical contents associated with topography and palustrine and fluvial processes.

Gypsum, carbonate and organic matter are paleoclimate indicators spectrally recorded by the imagery in the VIS-NIR. Saline soils with gypsum both on occasionally overflooded areas adjacent to shallow river channels and on mudflats around standing water pools, have been recorded by the imagery. Originally deeper areas rich in organic matter where marshes develop at times of low water movement are also shown.

Gypsum masks the presence of carbonate on the spectral response. Only X-ray diffraction analysis has depicted the presence of carbonate when coexisting with gypsum. Therefore, carbonate may also be present in the geochemically central fluvio-lacustrine areas rich in gypsum.

DAIS hyperspectral imagery has been able to distinguish four morphological units descending towards a receding wetland due to differential iron bearing minerals associated with variable time of exposure to the atmosphere and weather conditions. Mineralogical variations on iron oxides and hydroxides developed when sediments are emerged are easily recorded in the visible wavelength range.

The older units rich in hematite and poor in carbonate depict a distinguishing convex shape in the visible with a shoulder at 850 nm due to the ferric ion from hematite. On the contrary, the younger less dehydrated units, display a smooth depression between 700-740 nm due to goethite, and a subtle absorption or flattened response at 2300 nm because of the presence of carbonate. Both features are displayed by imagery and laboratory spectra.

DAIS thermal infrared, particularly sensitive to topography, was first used to depict spectrally variable areas. From them, through successive hyperspectral image processing on selectively masked areas, a spatial map of the paleolake has been drawn from the imagery, orientating drill location for further palinological studies and paleoenvironmental analysis.

## ACKNOWLEDGEMENT

The Fifth Framework Program, Improvement of Human Potential, Access to Research Infrastructures (contr. HPRI-CT-1999-00075, ref HS2000-ES1) funded data for this work. Thanks are due to S. Martin Alfageme and Iñigo Martin for software and hardware assistance (STIG, University of Salamanca). J. O´Malley reviewed the English version.

## REFERENCES

[1] ABRAMS, M.J., ASHLEY, R.P., ROWAN, L.C., GOETZ, A.F.H. AND KAHLE, A.B., 1977: Mapping of hydrothermal alteration in the Cuprite mining district Nevada, using aircraft scanner images for the spectral region 0.46 to 2.36 μm. *Geology, 5*, pp. 713-718.

[2] ABRAMS, M., ABBOTT, E. AND KAHLE, A., 1991: Combined Use of Visible, Reflected Infrared, and Thermal Infrared Images for Mapping Hawaiian Lava Flows. *Journal of Geophysical Research, 96- B1*, pp. 475-484.

[3] ALLEN , P.A. AND COLLINSON, J.D., 1978: Lakes. In: Reading, H.G. (ed.): Sedimentary Environment and Facies, pp 63-282. Blackwell Scientific Publications, Oxford, London.

[4] AMOS, B.J., AND GREENBAUM, D., 1989: Alteration detection using TM imagery. The effects of supergene weathering in an arid climate. *International Journal of Remote Sensing, 10-3*, pp. 515-527.

[5] ARAUZO, M., RUBIO, A., AND VICIOSO, J., 1996: El ambiente acuático: Hidroquímica. In :Alvarez Cobelas, M. y Cirujano, S., (ed.), Las Tablas de Daimiel, Ecología Acuática y Sociedad, pp. 70-90. Organismo Autónomo Parques Nacionales, Madrid.

[6] BOARDMAN, J. W., 1993: Automated spectral unmixing of AVIRIS data using convex geometry. *Proc. Fourth JPL Airborne Geoscience Workshop 1993*, JPL Publication 93-26, 1, pp. 11 - 14.

[7] BOARDMAN J.W. AND KRUSE, F. A., 1994: Automated spectral analysis: A geologic example using AVIRIS data, north Grapevine Mountains, Nevada. *Proc. Tenth Thematic Conference on Geologic Remote Sensing 1994*, pp. I-407 - I-418.

[8] BUCKINGHAM, W.F. AND SOMMER S.E., 1983: Mineralogical characterization of rock surfaces formed by hydrothermal alteration and weathering. Application to remote sensing, *Economic Geology, 78*, pp. 664-674.

[9] CASADO, S. AND MONTES, C., 1995: Guía de los lagos y humedales de España. Reyero, Madrid.

[10] CLARK, R. N., SWAYZE, G. A., GALLAGHER, A., KING, T. V. V. AND CALVIN, W. M., 1993: The U.S. Geological Survey Digital Spectral Library: Version 1: 0.2 to 3.0 mm. U.S. Geological Survey, Open File Report 93-592, Reston, USA.

[11] CROWLEY, J.K. AND HOOK, S.J., 1996: Mapping playa evaporite minerals and associated sediments in Death Valley, California, with multispectral thermal infrared images. *Journal of Geophysical Research, 101-B1*, pp. 643-660.

[12] CROWLEY, J.K., 1991: Visible and near-infrared (0.4-2.5 (m) reflectance spectra of playa evaporite minerals. *Journal of Geophysical Research, 96*, pp. 16.231-16.240.

[13] CROWLEY, J.K., 1986: Visible and Near-Infrared Spectra of Carbonate Rocks: Reflectance Variations Related to Petrographic Texture and Impurities. *Journal of Geophysical Research, 91-B5*, pp. 5001-5012.

[14] DE JONG, S.M., 1992: The Analysis of Spectroscopical Data to Map Soil Types and Soil Crusts of Mediterranean Eroded Soils. *Soil Technology, 5*, pp. 199-211.

[15] DEHAAN, R.L. AND TAYLOR, G.R., 2002: Field-derived spectra of salinized soils and vegetation as indicators of irrigation-induced soil salinization. *Remote Sensing of Environment 80*, pp. 406-417.

[16] DUCHAUFOUR, PH., 1984: Edafogénesis y Clasificación. Masson, Barcelona.

[17] CROWLEY, J.K., 1993, Mapping playa evaporite minerals with AVIRIS data: A first report from Death Valley, California. *Remote Sensing of Environment, 44*, pp. 337-356.

[18] EL BAZ, F., 1978: The meaning of desert color in earth orbital photographs. *Photogrametric Engineering and Remote Sensing, 44*, pp. 69-75.

[19] EL BAZ, F., PRESTEL, D.J., 1980: Desert varnish on sand grains from the Western Desert of Egypt: Importance of the clay component and implications to Mars. In : Lunar and Planetary Science (ed.): Lunar and Planetary Science XI, pp. 254-256. Houston, Texas.
[20] FARRAND, W.H., 1997: Identification and mapping of ferric oxide and oxyhydroxide minerals in imaging spectrometer data of Summitville, Colorado, U.S.A., and the surrounding San Juan Mountains. *International Journal of Remote Sensing, 18-7*, pp. 1543-1552.
[21] GAFFEY, S.J., 1986: Spectral reflectance of carbonate minerals in the visible and near infrared (0.35-2.55 microns): calcite, aragonite, and dolomite. *American Mineralogist, 71*, pp.151-162.
[22] GALVAO, L.S., AND VITORELLO, I., 1998: Role of organic matter in obliterating the effects of iron on spectral reflectance and colour of Brazilian tropical soils. *International Journal of Remote Sensing, 19-10*, pp. 1969-1979.
[23] GARCÍA ANTÓN, M., MORLA, C., RUIZ ZAPATA, B., SAIS OLLERO, H., 1986: Contribución al conocimiento del paisaje vegetal Holoceno en la Submeseta Sur Ibérica: análisis polínico de sedimentos higroturbosos en el Campo de Calatrava (Ciudad Real, España). In: F. López Vera (ed.): Quaternary Climate in Western Mediterranean. Universidad Autónoma de Madrid, Madrid.
[24] GARCÍA-MELÉNDEZ, E., SUÁREZ, M., AND RIAZA, A., 2000: Discrimination of active alluvial sedimentary surfaces in TM images based on laboratory reflectance spectroscopy. *Proc. 19th EARSeL Symposium 1999*, pp. 497-500.
[25] GEGE, P., BERAN, D., MOOSHUBER, W., SCHULZ, J., VAN DER PIEPEN, H., 1998: System analysis and performance of the new version of the imaging spectrometer ROSIS. *Proc. 1st Workshop on "Imaging Spectroscopy" 1998*, pp. 29-36.
[26] GROVE, C. I., HOOK, S. J., AND PAYLOR II, E. D., 1992: Laboratory Reflectance Spectra of 160 Minerals, 0.4 to 2.5 Micrometers. Jet Propulsion Laboratory Pub., pp.92-2.
[27] HUNT, G.R., SALISBURY, J.W., 1971a: Visible and Near-infrared Spectra of Minerals and Rocks: II. Carbonates, *Modern Geology*, 2, 23-30.
[28] HUNT, G.R., SALISBURY, J.W., AND LENHOF, J., 1971b: Visible and Near-infrared Spectra of Minerals and Rocks: III Oxides and Hydroxides. *Modern Geology, 2*, pp. 191-205.
[29] HUNT, G.R. AND ASHLEY, R.P., 1979: Spectra of altered rocks in the visible and near-infrared. *Economic Geology, 74*, pp. 1613-1629.
[30] JARMER,T., LAVÉE, H., HILL, J., AND SARAH, P., 2000: Spectral detection of inorganic carbon content along a semi-arid to hyper-arid climatic gradient in the Judean Desert (Israel). *Proc. Second EARSeL Workshop on Imaging Spectroscopy 2000*, International Institute for Aerospace Sciences and Remote Sensing. Enschede, The Netherlands.
[31] KAHLE, A.B., A.R. GILLESPIE, E.A. ABBOTT, M. J. ABRAMS, R. E. WALKER AND G. HOOVER, 1988: Relative Dating of Hawaiian Lava Flows Using Multispectral Themal Infrared Images: A New Tool for Geologic Mapping of Young Volcanic Terranes. *Journal of Geophysical Research, 93-B12*, pp. 15239-15251.
[32] KELTS, K., AND HSÜ, K.J., 1978: Freshwater Carbonate Sedimentation. In :Lerman, A., (ed.): Lakes: chemistry, geology, physics. Springer Verlag, New York.
[33] KOCH, M., 2000: Geological controls of land degradation as detected by remote sensing: a case study in Los Monegros, north-east Spain. *International Journal of Remote Sensing, 21-3*, pp. 457-474.
[34] KRUSE, F. A., LEFKOFF, A. B., BOARDMAN, J. B., HEIDEBRECHT, K. B., SHAPIRO. A. T., BARLOON, P. J., AND GOETZ, A. F. H., 1993: The Spectral Imaging Processing System (SIPS) – Interactive Visualization and Analysis of Imaging Spectrometer Data. *Remote Sensing of Environment, 44*, pp. 145-163.
[35] LEONE, A.P., AND ESCADAFAL, R., 2001: Statistical analysis of soil colour and spectroradiometric data for hyperspectral remote sensing of soil properties (example in a southern Italy Mediterranean ecosystem), *International Journal of Remote Sensing, 22-12*, pp. 2311-2328.
[36] LLAMAS, M.R., 1988: Conflicts Between Wetland Conservation and Groundwater Exploitation: Two Case Histories in Spain. *Environmental Geology and Water Science, 11-3*, pp. 241-251.
[37] LOGAN, R.F., 1960: The Central Namib Desert.National Research Council Publication 785.
[38] LYON, R.S.P., 1997: Weathering products and other coatings on rock surfaces: problems with airborne scanner imagery (RSS97-112). *Proc. 23rd Annual Conference and Exhibition of the Remote Sensing Society 1997*, pp. 54-59.
[39] MADEIRA, J., BEDIDI, A., CERVELLE, B., PUGET, M., FLAY, N., 1997: Visible spectrometric indices of hematite (Hm) and goethite (Gt) content in lateritic soils: the application of a Thematic Mapper (TM) image for soil-mapping in Brasilia, Brazil. *International Journal of Remote Sensing, 18-13*, pp. 2835-2852.
[40] MATHIEU, R., POUGET, M., CERVELLE, B. AND ESCADAFAL, R., 1998: Relationships between Satellite-Based Radiometric Indices Simulated Using Laboratory Reflectance Data and Typic Soil Color of an arid Environment. *Remote Sensing of Environment, 66*, pp. 17-28.

[41] McCAY, D., CONSTANTONOPOLUS, C., PRESTEL, DJ. AND EL BAZ, F., 1980: Thickness of coatings on quartz grains from the Great Sand Sea, Egypt. In Reports of Planetary Geology Program- 1980, Washington D.C.: National Aeronautics and Research Administration, NASA TM-82385, 1980, 304-306.
[42] MUNSELL, COLOR CO. ,1950, revisado 1990: Munsell Soil Color Charts, Munsell Color, Macbecth Division of Kollmorgen Corporation, Baltimore, MD.
[43] PÉREZ GONZÁLEZ, A., ALEIXANDRE, A., PINILLA, J., Y GALLARDO, J., 1983: El pasaje eólico de la llanura aluvial de San Juan (llanura manchega central), *Proc. VI Reunión del Grupo Español de Trabajo en el Cuaternario 1983*, pp. 631-655.
[44] PONTUAL, A., 1987: The effect of weathering minerals on the spectral response of rocks in Landsat Thematic Mapper imagery, *Proc. 13th Annual Conference of the Remote Sensing Society 1987*, pp. 549-558.
[45] PORTERO GARCÍA, J.M., ANCOCHEA, E., Y GALLARDO, J., 1988: Memoria del Mapa Geológico a escala 1:50.000, Segunda Serie, hoja nº 760 (Daimiel). Instituto Geológico y Minero de España, Madrid.
[46] POTTER, T.R. AND ROSSMAN, J.R., 1977: Desert varnish: the importance of clay minerals. *Science, 196*, pp. 1446-1448.
[47] RIAZA, A., 1992: Reflectancia en rocas en función de su litología y fábrica interna. II Cartografía de rocas ígneas en el Complejo de Burguillos del Cerro en el visible y el infrarrojo cercano: reflectancia espectral en el laboratorio y evaluación estadística de la misma en relación con imágenes thematic mapper. *Boletín Geológico y Minero, 103*, n.3, 3-26.
[48] RIAZA, A., MEDIAVILLA, R., SANTISTEBAN, J. L., VILLAR, P. AND MARTÍN ALFAGEME, S., 1995: Regolitos en una cuenca terciaria. Propiedades espectrales según su mineralogía en función de la evolución climática, *Proc. Coloquio Internacional sobre propiedades espectrales y teledetección de los suelos y rocas del visible al infrarrojo medio 1995*. pp. 100-104.
[49] RIAZA, A., MEDIAVILLA, R., SANTISTEBAN, J. L., VILLAR, P. AND MARTÍN ALFAGEME, S., 1997: Cartografía de formaciones geológicas litológicamente similares en zonas llanas cultivadas, *Proc. V Reunión Científica de la Asociación Española de Teledetección 1993*. pp. 863-876.
[50] RIAZA, A., KAUFMANN, H., ZOCK, A. AND MÜLLER, A., 1998: Mineral Mapping in Maktesh_Ramon (Israel) using DAIS 7915. *Proc. 1st EARSeL Workshop on Imaging Spectroscopy 1998*, pp. 365-374.
[51] RIAZA, A., MEDIAVILLA, R., AND SANTISTEBAN, J.I., 2000: Mapping geological stages of climate-dependent iron and clay weathering alteration and lithologically uniform sedimentary units using Thematic Mapper imagery, *International Journal of Remote Sensing. 21-5*, pp. 937-950.
[52] RIAZA, A., STROBL, P., MÜLLER, A., BEISL, U., AND HAUSOLD, A., 2001: Spectral mapping of rock weathering degrees on granite using hyperspectral DAIS 7915 Spectrometer Data. *International Journal of Applied Earth Observation and Geoinformation, Special issue: Applications of imaging spectroscopy, 3-4*, pp. 345-354.
[53] RIAZA, A., MEDIAVILLA, R., GARCÍA-MELÉNDEZ, E., SUÁREZ, M., HAUSOLD, A., BEISL, U., VAN DER WERFF, H., 2002: Mapping paleoflooded areas on evaporite playa deposits over sandy sediments (Tablas de Daimiel, Spain) using hyperspectral DAIS 7915 and ROSIS Spectrometer data. In: José A. Sobrino (ed.): Recent Advances in Quantitative Remote Sensing, pp. 371-379.
[54] RIAZA, A., GARCÍA-MELÉNDEZ, E., SUÁREZ, M., HAUSOLD, A., BEISL, U., VAN DER WERFF, H., 2003: Semi-Arid Iron Bearing Red Sands On Emerged Areas Around Lake Marshes (Tablas De Daimiel, Spain) Using Hyperpestral Dais 7915 And Rosis Spectrometer Data. *Proc. Workshop on Airborne Remote Sensing for Geosphysical and Environmental Applications 2003*, in press.
[55] RICHTER, R., 1996: Atmospheric correction of DAIS hyperspectral image data. *Computers & Geosciences, 22-7*, pp. 785-793.
[56] RICHTER, R., MÜLLER, A. AND HEIDEN, U., 2002: Aspects of operational atmospheric correction of hyperspectral imagery. *International Journal of Remote Sensing, 23-10*, pp. 145-158.
[57] RIVARD, B., ARVIDSON, R.E., DUNCAN, I.J., SULTAN, M. AND EL KALIOUBY, B., 1992: Varnish, sediment and rock controls on spectral reflectance of outcrops in arid regions, *Geology, 20*, 295-298.
[58] RODRIGUEZ GARCÍA, J.A., 1998: Geomorfología de las Tablas de Daimiel y del endorreismo manchego centro-occidental. October 1998, MSc Thesis, University Complutense of Madrid, 164 p, unpublished.
[59] ROWAN, L.C., WETLAUFER, P.H., GOETZ, A.F.H., BILLINGSLEY, F.C. AND STEWART, J.H., 1976: Discrimination of Rock Types and Detection of Hydrothermally Altered Areas in South Central Nevada by the Use of Computer Enhanced ERTS Images. United States Geological Survey Professional Paper, 883.
[60] ROWAN, L.C., GOETZ, A.F.H. AND ASHLEY, R.P., 1977: Discrimination of Hydrothermally Altered and Unaltered Rocks in the Visible and Near Infrared Multispectral Images. *Geophysics, 42-3*, pp. 522-535.
[61] SALISBURY, J.W., WALTER, L.S., VERGO, N. AND D´ARIA, D. M., 1992: Infrared (2.1-25 μm) Spectra of Minerals. The John Hopkins University Press.
[62] SEGAL, D.B., 1982: Theoretical basis for differentiation of ferric-iron bearing minerals using Landsat MSS data. *Proc. International Symposium on Remote Sensing of Environment, 2nd Thematic Conference, Remote*

*Sensing for Exploration Geology 1982, II*, pp. 949-951.
[63] SEGAL, D.B., 1983: Use of Landsat Multispectral Scanner Data for the Definition of Limonitic Exposures in Heavily Vegetated Areas,.*Economic Geology, 78*, pp. 711-722.
[64] SHIELDS, J.A., PAUL, E. A., ARNAUD, R.J.SR. AND HEAD, W.K., 1968: Spectrophotometric measurement of soil color and its relationship to moisture and organic matter. *Canadian Journal of Soil Science, 48*, pp. 271-280.
[65] STROBL, P., RICHTER, R., LEHMAN, F., MÜLLER, A., ZHUKOV, B., AND OERTEL, D., 1996: Preprocessing for the Digital Airborne Imaging Spectrometer DAIS 7915. *Proc. SPIE´s AEROSENSE Conference 1996, 2758*, pp. 375-382.
[66] TOWNSEND, T.E., 1987: Discrimination of iron alteration Minerals in Visible and Near-Infrared Reflectance Data. *Journal of Geophysical Research, 92 (B2)*, pp. 1441-1454.
[67] WALKER, T.R., 1967: Formation of red beds in modern and ancient deserts. *Geological Society of America Bulletin, 78*, pp. 353-368.
[68] WHITE, K., LIVINGSTONE, I., , GURNEY, S., DEARING, J., AND BATEMAN, M., 2000: Post-processing of mineral proportions maps derived from Landsat Thematic Mapper data for mapping surficial materials: the example of the Matmata Loess. *Proc. 26th Annual Conference of The Remote Sensing Society, 2000*, CD-R University of Leicester.
[69] WICKERSHEIM, K.A., AND LEFEVER, R.A., 1968: Absorption Spectra of Ferric Iron-Containing Oxides. *The Journal of Chemical Physics, 36-3*, pp. 844-850.
[70] YOUNIS, M.T., GILABERT, A.A., AND MELIÁ, J., 1997: Weathering process effects on spectral reflectance of rocks in a semi-arid environment, *International Journal of Remote Sensing, 18-16*, pp. 3361-3377.